Published in final edited form as:
Biomaterials. 2008 July ; 29(19): 2849–2857. doi:10.1016/j.biomaterials.2008.03.036.

The effect of integrin-specific bioactive coatings on tissue healing and implant osseointegration

Timothy A. Petrie[1,2], **Jenny E. Raynor**[3], **Catherine D. Reyes**[1,2], **Kellie L. Burns**[1,2], **David M. Collard**[3], and **Andrés J. García**[1,2]

1 *Woodruff School of Mechanical Engineering, Georgia Institute of Technology, Atlanta, GA 30332*

2 *Petit Institute for Bioengineering and Bioscience, Georgia Institute of Technology, Atlanta, GA 30332*

3 *School of Chemistry and Biochemistry, Georgia Institute of Technology, Atlanta, GA 30332*

Abstract

Implant osseointegration, defined as bone apposition and functional fixation, is a requisite for clinical success in orthopaedic and dental applications, many of which are restricted by implant loosening. Modification of implants to present bioactive motifs such as the RGD cell-adhesive sequence from fibronectin (FN) represents a promising approach in regenerative medicine. However, these biomimetic strategies have yielded only marginal enhancements in tissue healing *in vivo.* In this study, clinical-grade titanium implants were grafted with a non-fouling oligo(ethylene glycol)-substituted polymer coating functionalized with controlled densities of ligands of varying specificity for target integrin receptors. Biomaterials presenting the $\alpha_5\beta_1$-integrin-specific FN fragment $FNIII_{7–10}$ enhanced osteoblastic differentiation in bone marrow stromal cells compared to unmodified titanium and RGD-presenting surfaces. Importantly, $FNIII_{7–10}$-functionalized titanium significantly improved functional implant osseointegration compared to RGD-functionalized and unmodified titanium *in vivo*. This study demonstrates that bioactive coatings that promote integrin binding specificity regulate marrow-derived progenitor osteoblastic differentiation and enhance healing responses and functional integration of biomedical implants. This work identifies an innovative strategy for the rational design of biomaterials for regenerative medicine.

1. Introduction

Over 713,000 joint arthroplasties, mostly hip and knee procedures in arthritic patients, at a cost of $15 billion were performed in the U.S. in 2000 [1]. Even though artificial joint replacements can function properly for a decade, the long-term success of arthroplasties is limited by implant loosening and wear, often resulting in patient discomfort and pain and requiring revision surgery [2]. More importantly, the lifetime of these implants must increase as the number of younger patients needing joint replacements continues to steadily increase [3]. Considerable efforts have focused on implant surface technologies, particularly macro-and micro-porous coatings for bone ingrowth and bone-bonding ceramic coatings, to promote early integration into the surrounding bone [4]. However, inadequate cell-material interactions leading to slow

Corresponding Author: Andrés J. García, Woodruff School of Mechanical Engineering, 315 Ferst Drive, Room 2314 IBB, Atlanta, GA 30332-0363, andres.garcia@me.gatech.edu, Phone: 404-894-9384, Fax: 404-385-1397.

rates of osseointegration and poor mechanical properties currently restrict these approaches [5].

Cell-biomaterial interactions govern host responses to implanted devices, integration of biomedical prostheses and tissue-engineered constructs, and the performance of biotechnological supports [6–8]. In most instances, cells recognize and adhere via integrin receptors to biomacromolecules that adsorb non-specifically onto synthetic surfaces [9]. Integrins are a widely expressed family of heterodimeric (αβ) transmembrane receptors that provide anchorage forces and trigger signals regulating cell survival, proliferation, and differentiation, often overlapping with other receptor pathways [10]. For example, α_V-containing integrins are essential for steroid hormone and growth factor induction of osteoblast differentiation. [11,12] Because of the central roles of integrin-mediated adhesion in tissue formation, maintenance, and repair, recent bio-inspired biomaterial strategies have focused on presenting integrin ligands such as extracellular matrix proteins and short bioadhesive motifs derived from these components on implant surfaces [13]. The most common approach relies on the presentation of the arginine-glycine-aspartic acid (RGD) adhesive sequence derived from FN. While synthetic and natural materials functionalized with RGD oligopeptides support integrin-mediated adhesion, proliferation, and differentiation *in vitro*, mounting evidence indicates that this biomaterial surface engineering strategy does not enhance biomedical implant integration or function in rigorous animal models [14–16]. Based on previous *in vitro* work demonstrating that integrin binding specificity ($\alpha_5\beta_1$ vs. $\alpha_V\beta_3$) regulates osteoblastic differentiation [17], we hypothesized that the marginal healing responses to RGD-functionalized implants arise from the lack of selectivity of this ligand for specific integrins. In the present study, we used a novel polymer brush system to analyze mechanistically the effect on *in vitro* osteogenic stromal cell differentiation and bone tissue healing for clinical-grade titanium functionalized with ligands with varying specificity for target integrin receptors. We demonstrate that biomaterial coatings specific for integrin adhesion receptors regulate osteoblastic differentiation of marrow-derived progenitor cells and enhance bone tissue healing and the functional integration of clinically-relevant biomedical implants.

2. Materials and methods

2.1. Poly(OEGMA) polymer brush preparation and peptide tethering on titanium

Polymeric brushes, which are arrays of polymer chains attached at one end to a surface, on titanium substrates were synthesized by surface-initiated atom-transfer radical polymerization of poly(oligo(ethylene glycol) methacrylate) (poly(OEGMA)) [18]. Titanium-coated glass slides or custom-made commercially pure titanium implants were incubated in a 1:1 solution of chlorodimethyl(11-(2-bromo-2-methylpropionyloxy)undecyl)silane and dodecyldimethylchlorosilane in anhydrous hexane. Poly(OEGMA) brushes were polymerized by immersion into a solution of OEGMA (28.3 mmol), CuBr (1.6 mmol), 2,2'-dipyridyl (2.8 mmol) in a 1:4 mixture of MeOH and H_2O for 4 h. The resulting polymer brushes were 135 Å as determined by ellipsometry. For ligand tethering, brushes were first incubated in 4-nitrophenyl chloroformate (1.4 mmol in THF), which "activates" the brushes for subsequent ligand tethering by replacing a portion of the hydroxyl groups situated at the end of the polymer brushes with nitrophenyl chloroformate (NPC). The "activated" NPC-terminated brushes are then susceptible to attack and replacement by primary amine groups on bioadhesive peptides or proteins. Likewise, the activated brushes are then incubated in $FNIII_{7–10}$ or RGD in PBS for 30 min to allow ligand tethering, and residual activated NPC sites were quenched in 20 mM glycine in PBS. $FNIII_{7–10}$ was expressed in *E. coli* and purified [19], and the linear RGD oligopeptide (GRGDSPC) was purchased from BACHEM. Brush synthesis and functionalization reactions were verified by XPS (X-ray spectroscopy) and FTIR (Fourier Transform infrared spectroscopy). Ligand surface density measurements were obtained via

surface plasmon resonance using a Biacore X instrument.. Antibody-based bioactivity assay was performed by ELISA using HFN7.1 antibody.

2.2. Cell adhesion and integrin binding assays

Rat bone marrow stromal cells were isolated and cultured under IACUC-approved procedures [20]. Cell adhesion to engineered surfaces under serum-free conditions was measured at 1 h at 37°C using a centrifugation assay [21]. For integrin blocking, cells (passage 3 or less) were incubated in blocking antibodies (anti-rat CD49e [HMα5–1] or anti-rat CD51, BD Biosciences) for 20 min prior to cell seeding. Integrin binding was quantified using a crosslinking/extraction/reversal procedure using DTSSP crosslinker [22]. For FAK activation assays, cells were plated in the presence or absence of integrin-blocking antibodies on engineered substrates for 2 h at 37°C under serum-free conditions. Cells were lysed in RIPA buffer (1% Triton X-100, 1% sodium deoxycholate, 0.1% SDS, 150 mM NaCl, 150 mM Tris-HCl (pH 7.2), 350 μg/ml PMSF, 10 μg/ml leupeptin, and 10 μg/ml aprotonin), equal amounts of total protein loaded on 8% SDS-PAGE gels, separated by SDS-PAGE, and transferred to nitrocellulose membranes. FAK activation was assessed by subsequent western blotting using antibodies specific for FAK phosphotyrosines and normalized to total FAK.

2.3 Osteoblastic differentiation assays

Rat bone marrow stromal cells at low passage (3 or less) were seeded on appropriate surfaces at 100 cells/mm^2 in growth medium. After 24 h, cultures were maintained in osteogenic medium consisting of growth medium supplemented with 50 μg/ml-ascorbic acid and 3 mM sodium ß-glycerophosphate. Total RNA was isolated at 7 days after initial cell seeding, and gene expression was analyzed by RT-PCR using osteoblast-specific primers and normalized to a standard curve [20]. Alkaline phosphatase activity was quantified at 7 days after cell seeding using a fluorescence-based enzymatic assay [20]. Calcium content was determined using a commercial arsenazo III-containing Calcium Reagent kit (Diagnostic Services Ltd).

2.4. Implantation procedure and analysis

Implantations into the tibiae of mature Sprague-Dawley male rats were conducted in accordance with an IACUC-approved protocol as described previously [20]. Animals were euthanized after 4 weeks, and proximal tibiae were fixed in neutral buffered formalin for histology or recovered without fixation and maintained in PBS-moistened gauze for immediate mechanical testing. For histology, fixed tibiae were embedded in poly(methyl methacrylate), ground (50–80 μm), and stained with Sanderson's Rapid Bone Stain™ and a van Gieson counter stain. Bone implant contact was measured as the percentage of implant's circumference that was in direct contact with bone tissue. Implant mechanical fixation to the bone was measured with a pull-out force test using an EnduraTEC Bose ELF 3200 biomechanical testing apparatus [20]. Tests were performed at a constant force rate of 0.2 N/sec parallel to the long axis of the implant. The pull-out force was the maximum load achieved before failure.

2.5. Statistics

Data are reported as mean ± standard error. Results were analyzed by one-way ANOVA using SYSTAT 8.0 (SPSS). If treatment level differences were determined to be significant, pair-wise comparisons were performed using a Tukey post-hoc test. A 95% confidence level was considered significant.

3. Results

3.1. Bio-functionalized implant coatings to convey integrin binding specificity

In order to develop a robust coating for tunable presentation of bioactive factors on a clinically-relevant material, we designed and synthesized a polymer brush system incorporating a physiologically stable, non-fouling (resists protein adsorption) oligo(ethylene glycol)-substituted polymer brushes on clinical-grade titanium supports and functionalized the polymer coating with controlled densities of bioadhesive ligands.

We employed a "grafting from" approach based on surface-initiated atom-transfer radical polymerization (SI-ATRP) of poly(OEGMA) brushes on titanium [18] (Fig. 1A). Briefly, a 1:1 mixed self-assembled monolayer (SAM) of bromine-terminated initiator and unreactive, methyl-terminated co-adsorbate was formed on a clean titanium surface. The terminal bromine served as the radical initiator for the subsequent SI-ATRP of oligo(ethylene glycol) monomer to form thick, dense poly(OEGMA) brushes (Fig. 1B-1,2). The hydroxyl groups at the termini of the oligo(ethylene glycol) side chains of poly(OEGMA) were converted to 4-nitrophenyl carbonate by treatment with 4-nitrophenyl chloroformate (NPC) and functionalized with bioadhesive ligands via a urethane linkage (Fig. 1B–3,4). The progress of the synthesis and ligand tethering was validated by comparison of spectra from X-ray photoelectron spectroscopy (XPS) and glancing angle Fourier transform infrared (FTIR) spectroscopy with spectra from previously published characterization of these poly(OEGMA) brushes [18]. Brush thickness was easily modulated by polymerization time as previously shown [18]. All poly (OEGMA) brushes used in this study were grown to a thickness of 135 Å.

Two bioadhesive ligands with different integrin specificities were examined: (i) the recombinant fragment $FNIII_{7–10}$, which presents the RGD motif in the 10^{th} type III repeat and the PHSRN synergy sequence in the 9^{th} type III repeat of FN in the correct structural context and exhibits high selectivity for integrin $\alpha_5\beta_1$ [19]; and (ii) a linear RGD oligopeptide (GRGDSPC) that primarily supports $\alpha_V\beta_3$-mediated adhesion and is considered the "gold" standard in the field [19]. Controlled surface densities of tethered ligands were obtained by treating the NPC-modified polymer brushes with varying concentrations of peptide (Fig. 2A). The differences in tethering efficiency between $FNIII_{7–10}$ and RGD can be attributed to significant differences in ligand size. Importantly, ligand densities adsorbed on control surfaces presenting unmodified poly(OEGMA) brushes were <5% of the density immobilized on the functionalized surfaces, demonstrating the non-fouling nature of the unmodified poly (OEGMA) brush.

We next assessed the *in vitro* bioresistance and adhesive capacity of unmodified poly (OEGMA) brushes and brushes with peptide tethered on titanium. Surfaces were incubated in serum-containing media for various times and subsequently challenged with osteoblastic cells for 1 h. In contrast to control unmodified titanium which supported high levels of cell adhesion and spreading, unmodified poly(OEGMA) brushes resisted cell adhesion for over 56 days (Fig. 2B). The unfunctionalized poly(OEGMA) brushes exhibited excellent bioresistance compared to commonly-used model self-assembled monolayers of tri(ethylene glycol)-functionalized alkanethiols on gold, which displayed loss of bioresistance by the 10-day time point in serum-containing media. Moreover, poly(OEGMA) brushes presenting either $FNIII_{7–10}$ or RGD supported levels of cell adhesion comparable to the unmodified titanium (Fig. 2B), demonstrating that the tethered ligand is in a bioactive form that supports adhesive activities. Furthermore, NPC-activated brushes which were quenched with glycine, and to which no ligand was added, supported minimal cell adhesion, verifying that surface activation does not affect the brush non-fouling nature (Fig. 2B). In addition, this data indicates that, after glycine quenching, effectively no NPC groups are available for tethering of serum proteins, which could have potentially reduced the specificity of the surface. Finally, we demonstrated surface

density-dependent increases in available $FNIII_{7–10}$ ligand using a receptor-mimetic antibody-based assay (Fig. 2C). Taken together, these results demonstrate a robust approach to coat clinical-grade titanium with non-fouling/bioresistant oligo(ethylene glycol)-substituted polymer brushes which can be functionalized with controlled densities of bioadhesive ligands.

In vitro evaluation of these engineered titanium surfaces was performed using primary rat bone marrow stromal cells since this heterogeneous population contains osteoprogenitors, and human bone marrow stromal cells are currently used in clinical applications. Cell adhesion was examined using a centrifugation assay that applies a controlled detachment force. To allow direct comparisons between ligand-tethered surfaces, an equimolar ligand density of 0.9 pmol/cm^2 was used; this value represents the highest ligand density that could be ascribed for both surfaces to be equimolar. Upon exposure to serum, high levels of cell adhesion were observed for polymer brushes modified with either $FNIII_{7–10}$ or RGD brushes, as well as unmodified titanium (which adsorbs RGD-containing adhesive proteins from serum) (Fig. 3A). Unmodified poly(OEGMA) brushes displayed background levels of adhesion, further illustrating the bioresistance of this system. Importantly, a blocking anti-α_5 antibody completely eliminated cell adhesion to $FNIII_{7–10}$-tethered surfaces ($p<0.005$), whereas an anti-α_v antibody had no effect, verifying the specificity of this surface for $\alpha_5\beta_1$ integrin. Conversely, a function-perturbing anti-α_v antibody eliminated adhesion to both RGD-tethered surfaces and serum-exposed unmodified titanium ($p<0.01$; Fig. 3A), indicating that adhesion to these surfaces is primarily mediated by the $\alpha_V\beta_3$ integrin. As a complementary test of integrin specificity, we quantified integrin binding using a biochemical cross-linking/extraction/reversal technique [22]. Consistent with the antibody blocking experiments, $FNIII_{7–10}$-tethered brushes supported significantly higher levels of bound $\alpha_5\beta_1$ integrin compared to RGD-tethered brushes and serum-exposed titanium ($p<0.01$; Fig. 3B). On the other hand, the RGD-tethered brushes and serum-exposed titanium supported higher levels of bound $\alpha_V\beta_3$ that the $FNIII_{7–10}$ support ($p<0.006$). We note that the crosslinking/extraction technique has been validated for integrin binding to extracellular matrix proteins and relies on crosslinking free amines on both the receptor and ligand. Because the tethered RGD has no free amine, we attribute the $\alpha_V\beta_3$ signal on the RGD surfaces to crosslinking of clustered integrin-RGD bonds that were not completely extracted. This observation is consistent with previous results for cells adhering to RGD-presenting self-assembled monolayers [19]. The possibility that RGD tethering altered the non-fouling character of the brushes to result in non-specific protein adsorption from serum is highly unlikely as SPR measurements demonstrated background protein adsorption to RGD-functionalized supports. Furthermore, minimal cell adhesion under serum conditions to NPC-activated, glycine-quenched brush surfaces verified that brushes presenting a non-adhesive amino acid residue retain their non-fouling nature (Fig. 2B). More importantly, the integrin-specific character of each specific surface treatment was demonstrated by the integrin-blocking adhesion results. Collectively, these data demonstrate that $FNIII_{7–10}$-functionalized titanium selectively supports $\alpha_5\beta_1$-mediated cell adhesion, whereas the RGD-tethered surface primarily binds $\alpha_V\beta_3$ integrin.

As a final demonstration of the integrin-specific nature of these engineered supports, we assessed FAK phosphorylation in the presence of integrin blocking antibodies. FAK is an intracellular signaling molecule involved in integrin-mediated signal transduction and the osteogenic differentiation pathway [23,24]. We used phosphotyrosine-specific antibodies to examine the activation state of three important tyrosines in FAK: Y397 (autophosphorylation site), Y576 (essential for maximal kinase activity), and Y861 (major Src phosphorylation site) (Fig. 3C). FAK Y397 and Y576 exhibited higher phosphorylation levels on $FNIII_{7–10}$-engineered surfaces compared to RGD-functionalized brushes and serum-exposed titanium ($p<0.01$), whereas Y861 phosphorylation was elevated for the RGD-functionalized and serum-exposed titanium relative to the $FNIII_{7–10}$-tethered surface ($p<0.03$). Moreover, blocking antibodies against α_5, but not β_3, reduced the levels of phospho-Y397 and Y576 on the

$FNIII_{7–10}$-presenting titanium ($p<0.04$). For the RGD-functionalized poly(OEGMA) brushes, only the anti-β_3 antibody reduced FAK phosphorylation ($p<0.05$). We postulate that these differences in integrin binding specificity and FAK activation modulate cell signaling pathways and higher order cellular activities.

3.2. Effects of integrin-specific implant surfaces in modulating osteoblastic differentiation and mineralization

We used quantitative RT-PCR to probe osteoblastic gene expression in 7-day cultures of bone marrow stromal cells cultured in osteogenic media to investigate effects of integrin binding specificity on osteoblastic differentiation. Expression levels of Runx2/Cbfa1, a transcription factor essential for osteoblastic differentiation and bone formation [25], were elevated on the $FNIII_{7–10}$-functionalized surface compared to brushes functionalized with equimolar densities of RGD ($p<0.03$; Fig. 4A). The late osteoblastic markers osteocalcin (OCN) and bone sialoprotein (BSP) also exhibited increased transcript levels on $FNIII_{7–10}$-tethered brushes relative to RGD-functionalized supports ($p<0.003$). Consistent with the gene expression results, $FNIII_{7–10}$-tethered surfaces displayed higher alkaline phosphatase activity than RGD-functionalized surfaces ($p<0.03$; Fig. 4B). Finally, matrix mineralization, as determined by calcium incorporation, was used as an end-point functional marker. $FNIII_{7–10}$-engineered titanium displayed a 2-fold enhancement in mineralization relative to the RGD-tethered supports ($p<0.01$; Fig. 4C). No differences were observed between RGD-functionalized brushes and serum-exposed unmodified titanium for any differentiation marker. Collectively, these results demonstrate that non-fouling brush surfaces presenting $FNIII_{7–10}$ to target $\alpha_5\beta_1$ integrin trigger enhance osteoblastic differentiation and mineralization in primary bone marrow stromal cells compared to RGD-tethered brushes and serum-treated titanium surfaces that support $\alpha_V\beta_3$ binding.

3.3. Effects of integrin specificity in modulating functional implant osseointegration *in vivo*

We quantified osseointegration of implants in a rat tibia cortical bone model [20] to evaluate the *in vivo* performance of the engineered titanium surfaces in bone healing. Importantly, this *in vivo* model provides a rigorous platform to evaluate implant coating function in a relevant orthopaedic setting. Two 2.0-mm diameter defects were drilled into the medial aspect of the proximal tibial metaphysis using a saline cooled drill. Tapered cylindrical implants (Fig. 5A) of clinical-grade titanium were press-fit into the cortical defects (Fig. 5B). Implants were machined with a tapered stop collar to ensure equivalent initial bone contact across all samples, and each implant had a small channel spanning the head to permit subsequent pull-out testing following explantation. Biomaterial surface treatments evaluated were (i) unmodified poly (OEGMA) brushes, (ii) unmodified titanium (as a reference to the current clinical treatment), and brushes modified with either (iii) $FNIII_{7–10}$ or (iv) RGD at equimolar ligand densities (0.9 pmol/cm^2). In addition, a small number of implants with varying densities of $FNIII_{7–10}$ were analyzed. All implants were well-tolerated, and no complications were encountered during the course of the study. Following four weeks of implantation, the rat tibiae were harvested and analyzed for bone-implant contact by histomorphometry and implant mechanical fixation by pull-out testing.

Histological sections revealed extensive and contiguous bone matrix around $FNIII_{7–10}$-functionalized titanium implants (Fig. 5C). Less bone tissue was observed around the unmodified poly(OEGMA) brushes, poly(OEGMA) brushes with RGD tethered, and reference unmodified titanium implants, and the tissue present displayed a more porous morphology (Fig. 5C). Histomorphometric analysis of histological sections demonstrated a 70% enhancement in bone-implant contact area for $FNIII_{7–10}$-functionalized implants compared to the RGD-tethered or unfunctionalized poly(OEGMA) brushes ($p<0.02$; Fig. 5D). Notably, the bone-implant contact area for the $FNIII_{7–10}$ group was significantly higher than that for the

unmodified clinical-grade titanium implant ($p<0.02$). No evidence of multi-nucleated cells, foreign body giant cells, or fibrous capsule was observed in any of the sections. These findings demonstrate that controlled presentation of the integrin-specific ligand $FNIII_{7–10}$ using our polymer brush strategy significantly enhances implant integration into the host bone compared to implants presenting RGD-functionalized poly(OEGMA) brushes and the current clinical standard (unmodified titanium).

Mechanical fixation was used as an outcome measure of functional osseointegration. Pull-out mechanical testing revealed significantly higher mechanical fixation of the $FNIII_{7–10}$-functionalized implants over all other groups ($p<0.03$; Fig. 5E**)**. Implants coated with unmodified poly(OEGMA) brushes generated the lowest amount of bone apposition and mechanical fixation, suggesting that the polymer brushes retain their non-fouling/bioresistant character *in vivo*. $FNIII_{7–10}$-functionalized implants exhibited a 3.0-fold enhancement in fixation over RGD-tethered implants ($p<0.009$) and approximately a 4-fold improvement compared to the unmodified poly(OEGMA) brush coating ($p<0.001$). Notably, there were no differences in bone apposition or mechanical fixation between RGD-functionalized and unmodified poly(OEGMA) implants, demonstrating that presentation of the linear RGD sequence has no effects on implant osseointegration. Unmodified titanium displayed higher fixation than the unfunctionalized poly(OEGMA) brush ($p<0.01$), but the pull-out force was not statistically different from the RGD-tethered surface. Remarkably, $FNIII_{7–10}$-functionalized titanium exhibited higher mechanical fixation that the unmodified titanium ($p<0.05$), indicating that this biomolecular engineering strategy outperforms the current clinical standard.

A major advantage of the poly(OEGMA) brush system described in this work is the ability to precisely control the presentation of tethered ligands. Increases in the density of tethered $FNIII_{7–10}$ yielded linearly proportional increases in available bioactive ligand *in vitro* (Figure 2d). We examined whether the density of tethered bioadhesive ligand modulated *in vivo* bone healing by implanting samples with varying tethered densities of $FNIII_{7–10}$. Mechanical fixation increased with $FNIII_{7–10}$ surface density, displaying linear increases at low surface densities and reaching a saturation limit at high densities (Fig. 5F). These results are accurately described by a simple hyperbolic relationship ($R^2 = 0.87$). This functional dependence is consistent with *in vitro* results for simple receptor-mediated phenomena such as adhesion strength [26]. To our knowledge, this is the first experimental study demonstrating finely tuned *in vivo* healing in response to engineered bioadhesive cues on material surfaces.

4. Discussion

The presentation of biological active factors on the surface of biomedical devices has emerged as a promising strategy to enhance host healing responses to implanted devices [6,11]. Nonetheless, these biomimetic approaches have elicited marginal improvements in *in vivo* functional performance [12–14]. We hypothesized that these marginal healing responses result from uncontrolled signaling responses at the tissue-implant interface arising from unregulated or sub-optimal integrin binding. While model biomaterial surfaces to control ligand presentation (e.g., self-assembled monolayers on gold or silicon) have been extensively studied, the development of robust coating technologies for tunable presentation of bioactive factors on materials approved for biomedical implantation has been particularly challenging. Recent bioactive implant surface treatments on Ti, including porous hydroxyapatite, collagen I, and calcium phosphate co-precipitated with various other biological ligands, have augmented aspects of bone healing compared to unmodified Ti in various animal models [27–29]. However, these strategies lack control over protein adsorption, ligand presentation and density, and surface stability. The utility of this brush system in this study is the level of precise control

over bioactive ligand density and presentation and cellular integrin interaction in a physiological environment.

In the present work, we grafted clinical-grade titanium implants with a robust non-fouling polymer coating functionalized with controlled densities of ligands of varying integrin specificity to examine the role of integrin binding specificity on tissue responses to implanted devices. Our results demonstrate that conferring integrin binding specificity to biomedical implants regulates the osteoblastic differentiation of bone marrow-derived progenitor cells and significantly enhances *in vivo* bone healing and implant functional osseointegration. This work provides the first experimental demonstration that *in vivo* healing response can be finely tuned by engineering bioadhesive cues on synthetic biomedical material surfaces, and provides novel insights into the role of integrin receptors in directing specific signaling pathways and osteogenic cell functions. Importantly, this biomolecular strategy is based on surface engineering a robust non-fouling polymer coating on clinical-grade titanium, and therefore is applicable to existing biomedical implants. The integrin-specific biomaterial surfaces significantly enhanced *in vivo* implant integration and fixation compared to the current clinical standard (unmodified titanium) as well as biomimetic RGD-based surface treatments. This integrin-specific enhancement of functional integration may be potentially even greater since the $FNIII_{7–10}$ surface density tethered to the polymer coating was below saturation. Given the central role of integrin receptors in the maintenance and repair of numerous tissues, we expect that this strategy of conveying integrin specificity will enhance healing responses and integration of other biomedical implanted devices.

We attribute the enhanced bone tissue formation and functional osseointegration of the $\alpha_5\beta_1$-specific titanium implants to increased recruitment of osteoprogenitor cells and differentiation into osteoblasts at the tissue-implant interface. As demonstrated in the *in vitro* analyses (Fig. 3), $\alpha_5\beta_1$-mediated adhesion upregulated osteoblastic gene and protein expression and matrix mineralization in marrow-derived progenitor cells. The $\alpha_5\beta_1$ integrin is the central fibronectin receptor, and its expression has been associated with increased mineralization of osteosarcoma and calvarial osteoblast cells [27]. This study provides further evidence for directed $\alpha_5\beta_1$-mediated osteogenic differentiation as well as additional associated signaling through specific residues of FAK. In addition to cells directly interacting with the bioadhesive ligands on the implant surface, paracrine factors secreted at the tissue-interface could contribute to the pro-osteogenic healing response by recruiting additional osteoprogenitors and/or promoting osteoblastic differentiation in neighboring cells.

No differences in bone-implant contact or functional osseointegration were observed between RGD-tethered and unmodified titanium implants. We attribute the suboptimal host healing responses to these implants to reduced osteoblastic differentiation and bone formation. These two surfaces present adhesive ligands that primarily bind $\alpha_V\beta_3$. Osteogenic cell adhesion to the short synthetic RGD is primarily mediated by this integrin (Fig. 2). Similarly, cell adhesion to the unmodified titanium is mediated by RGD-containing proteins (e.g., fibrinogen, vitronectin [30]) that adsorb non-specifically to titanium and support $\alpha_V\beta_3$-mediated adhesion. As demonstrated in the *in vitro* analyses (Fig. 3) and previous work (15), binding of $\alpha_V\beta_3$ suppresses osteoblastic differentiation. Moreover, $\alpha_v\beta_3$-overexpressing osteoblasts exhibited impeded mineralization capacity due to suboptimal integrin-matrix interactions, JNK activity, and matrix protein expression [31]. In addition to reduced osteoblastic differentiation, it is possible that presentation of $\alpha_V\beta_3$-selective ligands reduces overall bone formation by enhancing osteoclastic activity. Integrin $\alpha_V\beta_3$ is a major component of podosomes in the sealing zones of resorptive pits [32], and $\alpha_V\beta_3$ antagonists reduce bone resorption by reducing osteoclast activity [33–35]. However, we did not observe accumulation of multi-nucleated cells at the bone tissue-implant interface, suggesting that osteoclastic responses were not the dominant mechanism. Using the unique integrin-specific ligand presentation system in this

study, we have obtained mechanistic insights into the functional roles of integrins in directing osteogenic behavior of stem-like stromal cells both *in vitro*, and, for the first time, *in vivo*.

A major contribution of the present study is the application of a stable non-fouling polymer coating that can be precisely engineered to present bioactive factors as a general strategy to convey biofunctionality to existing clinical devices. This approach is directly translatable to metal oxides and ceramic materials, and the tethering scheme is amenable to other protein ligands, including growth factors, antibodies, and enzymes, as well as aminated nucleic acids, carbohydrates, and lipids. Moreover, we have established the high physiological stability of this polymer brush system, affording long-term direct *in vivo* functional comparison of bioactive ligands. Consequently, we have been able to demonstrate in this study an integrin-specific mechanism for the regulation of progenitor cell differentiation into osteoblasts and *in vivo* enhancement of bone healing and implant osseointegration.

5. Conclusion

Clinical-grade titanium implants were grafted with a non-fouling oligo(ethylene glycol)-substituted polymer coating functionalized with equimolar densities of either RGD peptide or $\alpha_5\beta_1$-integrin-specific FN fragment $FNIII_{7–10}$. Biomaterials presenting $FNIII_{7–10}$ supported enhanced $\alpha_5\beta_1$ integrin binding and osteoblastic differentiation in bone marrow stromal cells compared to unmodified titanium and RGD-presenting surfaces, which promoted primarily $\alpha_v\beta_3$ binding. Importantly, $FNIII_{7–10}$-functionalized titanium significantly improved functional implant osseointegration compared to RGD-functionalized and unmodified titanium *in vivo*. This work identifies a robust strategy that may be applicable to improve the biological performance of other biomedical devices and constructs for regenerative medicine.

Acknowledgements

This work was funded by the NIH (R01 EB-004496), Arthritis Foundation, and Georgia Tech/Emory NSF ERC on the Engineering of Living Tissues (EEC-9731643). T.A.P. acknowledges support from the Medtronic Foundation. The authors gratefully acknowledge Wasatch Histo Consultants for histology and M. Mathews for implant machining.

7. References

1. American Academy of Orthopaedic Surgeons. 2003. Arthroplasty and Total Joint Replacement Procedures: National Center for Health Statistics, 1991 to 2000 National Hospital Discharge Survey.
2. Pilliar RM. Cementless implant fixation–toward improved reliability. Orthop Clin North Am 2005;36:113–119. [PubMed: 15542130]
3. Arthritis Foundation. National Arthritis Action Plan: A Public Health Strategy. CDC Web Page (www cdc gov) 1999
4. Bauer TW, Schils J. The pathology of total joint arthroplasty. I. Mechanisms of implant fixation. Skeletal Radiol 1999;28:423–432. [PubMed: 10486010]
5. Bauer TW, Schils J. The pathology of total joint arthroplasty.II. Mechanisms of implant failure. Skeletal Radiol 1999;28:483–497. [PubMed: 10525792]
6. Lutolf MP, Hubbell JA. Synthetic biomaterials as instructive extracellular microenvironments for morphogenesis in tissue engineering. Nat Biotechnol 2005;23:47–55. [PubMed: 15637621]
7. Anderson JM. Biological responses to materials. Annu Rev Mater Res 2001;31:81–110.
8. Hubbell JA. Biomaterials science and high-throughput screening. Nat Biotechnol 2004;22:828–829. [PubMed: 15229544]
9. García AJ. Get a grip: integrins in cell-biomaterial interactions. Biomaterials 2005;26:7525–7529. [PubMed: 16002137]
10. Hynes RO. Integrins: bidirectional, allosteric signaling machines. Cell 2002;110:673–687. [PubMed: 12297042]

11. Cheng SL, Lou J, Wright NM, Lai CF, Avioli LV, Riew KD. In vitro and in vivo induction of bone formation using a recombinant adenoviral vector carrying the human BMP-2 gene. Calcif Tissue Int 2001;68:87–94. [PubMed: 11310352]
12. Cheng SL, Lai CF, Fausto A, Chellaiah M, Feng X, McHugh KP, Teitelbaum SL, Civitelli R, Hruska KA, Ross FP, Avioli LV. Regulation of alphaVbeta3 and alphaVbeta5 integrins by dexamethasone in normal human osteoblastic cells. J Cell Biochem 2000;77:265–276. [PubMed: 10723092]
13. Langer R, Tirrell DA. Designing materials for biology and medicine. Nature 2004;428:487–492. [PubMed: 15057821]
14. Schliephake H, Scharnweber D, Dard M, Rossler S, Sewing A, Meyer J, Hoogestraat D. Effect of RGD peptide coating of titanium implants on periimplant bone formation in the alveolar crest. An experimental pilot study in dogs. Clin Oral Implants Res 2002;13:312–319. [PubMed: 12010163]
15. Barber TA, Ho JE, De Ranieri A, Virdi AS, Sumner DR, Healy KE. Peri-implant bone formation and implant integration strength of peptide-modified p(AAM-co-EG/AAC) interpenetrating polymer network-coated titanium implants. J Biomed Mater Res A 2007;80:306–320. [PubMed: 16960836]
16. Elmengaard B, Bechtold JE, Soballe K. In vivo study of the effect of RGD treatment on bone ongrowth on press-fit titanium alloy implants. Biomaterials 2005;26:3521–3526. [PubMed: 15621242]
17. Keselowsky BG, Collard DM, García AJ. Integrin binding specificity regulates biomaterial surface chemistry effects on cell differentiation. Proc Natl Acad Sci U S A 2005;102:5953–5957. [PubMed: 15827122]
18. Raynor JE, Petrie TA, García AJ, Collard DM. Controlling cell adhesion to titanium: Functionalization of poly[oligo(ethylene glycol methacrylate] brushes with cell-adhesive peptides. Adv Mater 2007;19:1724–1728.
19. Petrie TA, Capadona JR, Reyes CD, García AJ. Integrin specificity and enhanced cellular activities associated with surfaces presenting a recombinant fibronectin fragment compared to RGD supports. Biomaterials 2006;27:5459–5470. [PubMed: 16846640]
20. Reyes CD, Petrie TA, Burns KL, Schwartz Z, García AJ. Biomolecular surface coating to enhance orthopaedic tissue healing and integration. Biomaterials 2007;28:3228–3235. [PubMed: 17448533]
21. Reyes CD, García AJ. A centrifugation cell adhesion assay for high-throughput screening of biomaterial surfaces. J Biomed Mater Res 2003;67A:328–333.
22. Keselowsky BG, García AJ. Quantitative methods for analysis of integrin binding and focal adhesion formation on biomaterial surfaces. Biomaterials 2005;26:413–418. [PubMed: 15275815]
23. Hanks SK, Ryzhova L, Shin NY, Brabek J. Focal adhesion kinase signaling activities and their implications in the control of cell survival and motility. Front Biosci 2003;8:d982–d996. [PubMed: 12700132]
24. Tamura Y, Takeuchi Y, Suzawa M, Fukumoto S, Kato M, Miyazono K, Fujita T. Focal adhesion kinase activity is required for bone morphogenetic protein–Smad1 signaling and osteoblastic differentiation in murine MC3T3-E1 cells. J Bone Miner Res 2001;16:1772–1779. [PubMed: 11585340]
25. Ducy P, Zhang R, Geoffroy V, Ridall AL, Karsenty G. Osf2/Cbfa1: a transcriptional activator of osteoblast differentiation. Cell 1997;89:747–754. [PubMed: 9182762]
26. Gallant ND, Michael KE, García AJ. Cell adhesion strengthening: contributions of adhesive area, integrin binding, and focal adhesion assembly. Mol Biol Cell 2005;16:4329–4340. [PubMed: 16000373]
27. Rammelt S, Heck C, Bernhardt R, Bierbaum S, Scharnweber D, Goebbels J, Ziegler J, Biewener A, Zwipp H. In vivo effects of coating loaded and unloaded Ti implants with collagen, chondroitin sulfate, and hydroxyapatite in the sheep tibia. J Orthop Res 2007;25:1052–1061. [PubMed: 17457829]
28. Wang H, Eliaz N, Xiang Z, Hsu HP, Spector M, Hobbs LW. Early bone apposition in vivo on plasma-sprayed and electrochemically deposited hydroxyapatite coatings on titanium alloy. Biomaterials 2006;27:4192–4203. [PubMed: 16618502]
29. Siebers MC, Wolke JG, Frank W, X, Leeuwenburgh SC, Jansen JA. In vivo evaluation of the trabecular bone behavior to porous electrostatic spray deposition-derived calcium phosphate coatings. Clin Oral Implants Res 2007;18:354–361. [PubMed: 17298493]

30. Kanagaraja S, Lundstrom I, Nygren H, Tengvall P. Platelet binding and protein adsorption to titanium and gold after short time exposure to heparinized plasma and whole blood. Biomaterials 1996;17:2225–2232. [PubMed: 8968516]

31. Cheng SL, Lai CF, Blystone SD, Avioli LV. Bone mineralization and osteoblast differentiation are negatively modulated by integrin alpha(v)beta3. J Bone Miner Res 2001;16:277–288. [PubMed: 11204428]

32. Nakamura I, Pilkington MF, Lakkakorpi PT, Lipfert L, Sims SM, Dixon SJ, Rodan GA, Duong LT. Role of alpha(v)beta(3) integrin in osteoclast migration and formation of the sealing zone. J Cell Sci 1999;112:3985–3993. [PubMed: 10547359]

33. Engleman VW, Nickols GA, Ross FP, Horton MA, Griggs DW, Settle SL, Ruminski PG, Teitelbaum SL. A peptidomimetic antagonist of the alpha(v)beta3 integrin inhibits bone resorption in vitro and prevents osteoporosis in vivo. J Clin Invest 1997;99:2284–2292. [PubMed: 9151803]

34. Hutchinson JH, Halczenko W, Brashear KM, Breslin MJ, Coleman PJ, Duong lT, Fernandez-Metzler C, Gentile MA, Fisher JE, Hartman GD, Huff JR, Kimmel DB, Leu CT, Meissner RS, Merkle K, Nagy R, Pennypacker B, Perkins JJ, Prueksaritanont T, Rodan GA, Varga SL, Wesolowski GA, Zartman AE, Rodan SB, Duggan ME. Nonpeptide alphavbeta3 antagonists. 8. In vitro and in vivo evaluation of a potent alphavbeta3 antagonist for the prevention and treatment of osteoporosis. J Med Chem 2003;46:4790–4798. [PubMed: 14561098]

35. Carron CP, Meyer DM, Engleman VW, Rico JG, Ruminski PG, Ornberg RL, Westlin WF, Nickols GA. Peptidomimetic antagonists of alphavbeta3 inhibit bone resorption by inhibiting osteoclast bone resorptive activity, not osteoclast adhesion to bone. J Endocrinol 2000;165:587–598. [PubMed: 10828842]

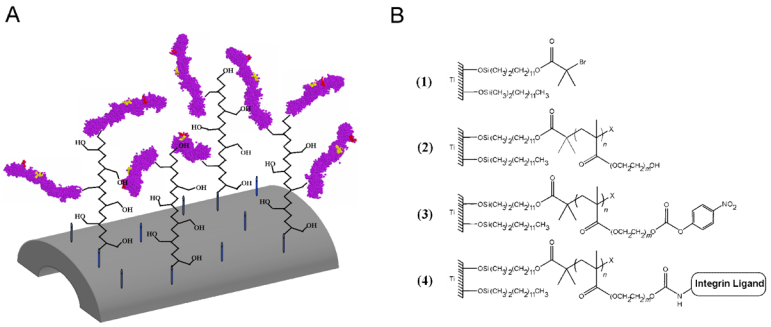

Figure 1.

Poly(OEGMA) brushes with ligand tethered on titanium. (A) Schematic of $FNIII_{7–10}$-tethered poly(OEGMA) brush system on titanium. Both linear RGD peptide and a fibronectin fragment $FNIII_{7–10}$ (purple) containing both the RGD (red) and PHSRN (yellow) sequence in the native ECM structural conformation were tethered to poly(OEGMA) brushes via NPC chemistry. Unactivated hydroxyl groups provided the non-fouling nature of the brushes. (B) Tethering scheme of integrin ligands to “activated” poly(OEGMA) brushes on titanium.

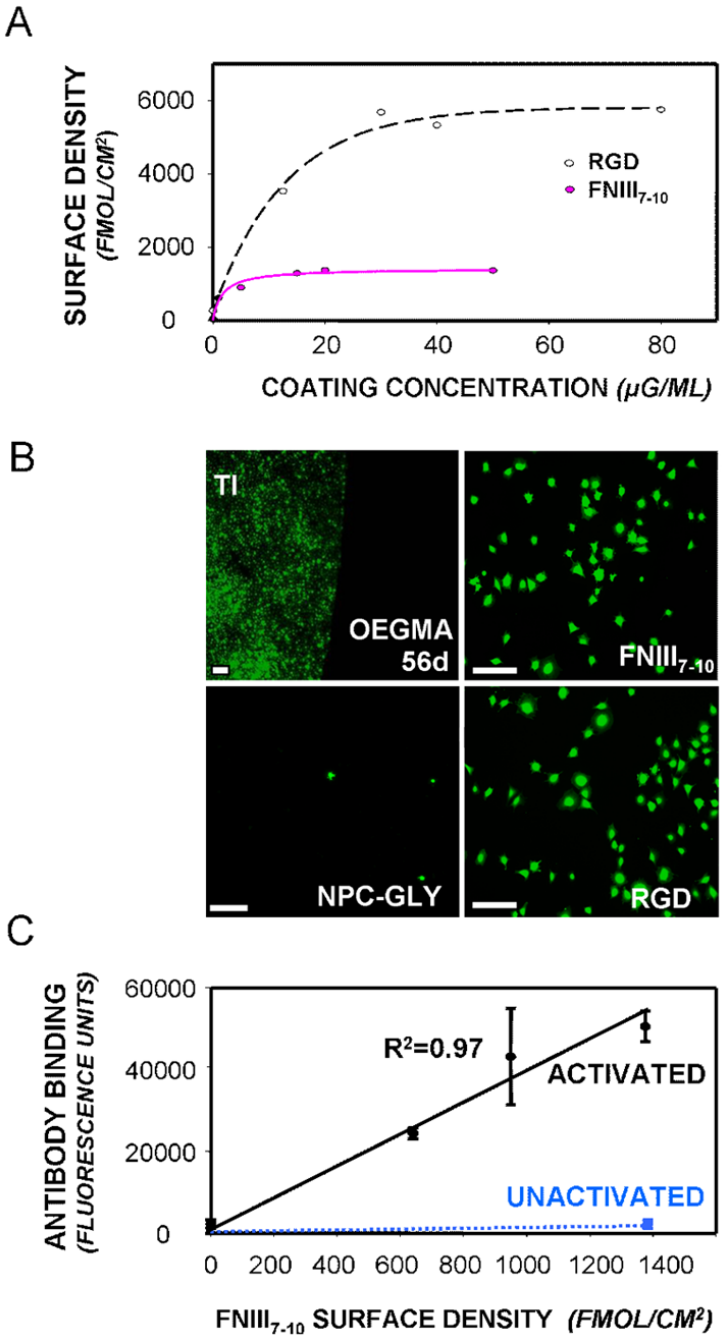

Figure 2.

Bioresistance and ligand tethering on poly(OEGMA) brushes on titanium. (A) Tethered densities of RGD and $FNIII_{7–10}$ on poly(OEGMA) brushes on titanium (hyperbolic curve fit, R^2=0.95). (B) *In vitro* bioresistance of poly(OEGMA) brushes on titanium to cell adhesion in serum-containing media. Cells were stained with green-colored calcein-AM (scale bar 100 μm). EG_3 SAMs were cell-resistant until day 10, while poly(OEGMA) brushes remained cell adhesion-resistant for at least 56 days. Cells adhered (1 h) and spread in serum-free conditions on $FNIII_{7–10}$-tethered and RGD-tethered brushes (0.9 pmol/cm^2) to the same extent as on serum-treated unmodified titanium. Cells did not adhere or spread in serum on NPC-activated brush surfaces quenched with glycine to which no bioadhesive ligand was added. (C)

Bioactivity and accessibility of $FNIII_{7–10}$ tethered to poly(OEGMA) brushes as determined by a receptor-mimetic antibody assay. $FNIII_{7–10}$ activity was detected on the NPC-modified poly (OEGMA) brushes (but not the unmodified brushes).

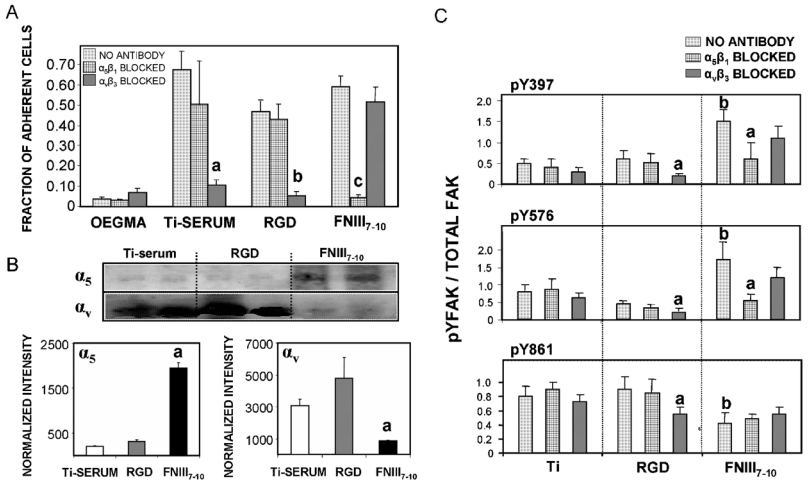

Figure 3.

Poly(OEGMA) brushes on titanium functionalized with integrin ligands display integrin specificity. (A) Bone marrow stromal cell adhesion to engineered surfaces is mediated by different integrin receptors as demonstrated by blocking antibodies. Ti-serum: a vs. no antibody control ($p<0.01$); RGD: b vs. no antibody control ($p<0.01$); $FNIII_{7–10}$: c vs. no antibody control ($p<0.005$). (B) Integrin binding analysis using a crosslinking/extraction/reversal procedure for stromal cells plated on ligand-tethered brush surfaces of equimolar density. α_5 :a vs. RGD, Ti-serum ($p<0.01$); α_V: a vs. Ti-serum ($p<0.006$). (C) FAK activation on equimolar ligand-tethered brush surfaces and serum-treated titanium is integrin-dependent. Relative levels of phospho-Y in FAK in the presence or absence of integrin blocking antibodies. Activation levels for Y397 and Y576 were higher on $FNIII_{7–10}$-tethered brushes than RGD-functionalized and Ti-serum supports (b; $p<0.01$). Y861 phosphorylation levels were reduced in $FNIII_{7–10}$-functionalized titanium relative to the other surfaces (b; $p<0.03$). Integrin blocking antibodies selectively reduced FAK phosphorylation. Y397: a vs. no antibody control ($p<0.04$); Y576: a vs. no antibody control ($p<0.05$); Y861: a vs. no antibody control ($p<0.05$).

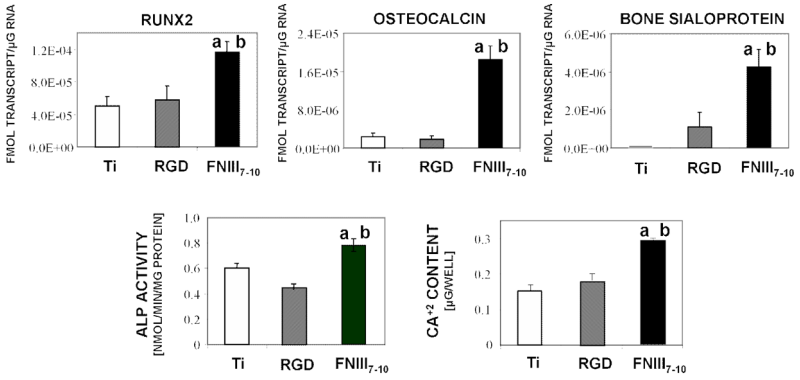

Figure 4.

$FNIII_{7–10}$-functionalized surfaces enhance osteoblastic differentiation and mineralization in bone marrow stromal cultures at 7 days. (A) Gene expression levels for Runx2 transcription factor, osteocalcin, and bone sialoprotein. a vs. RGD ($p<0.02$); b vs. Ti-serum ($p<0.02$). (B) Alkaline phosphatase activity. a vs. RGD ($p<0.01$); b vs. Ti-serum ($p<0.03$). (C) Calcium content. a vs. RGD ($p<0.01$); b vs. Ti-serum ($p<0.008$).

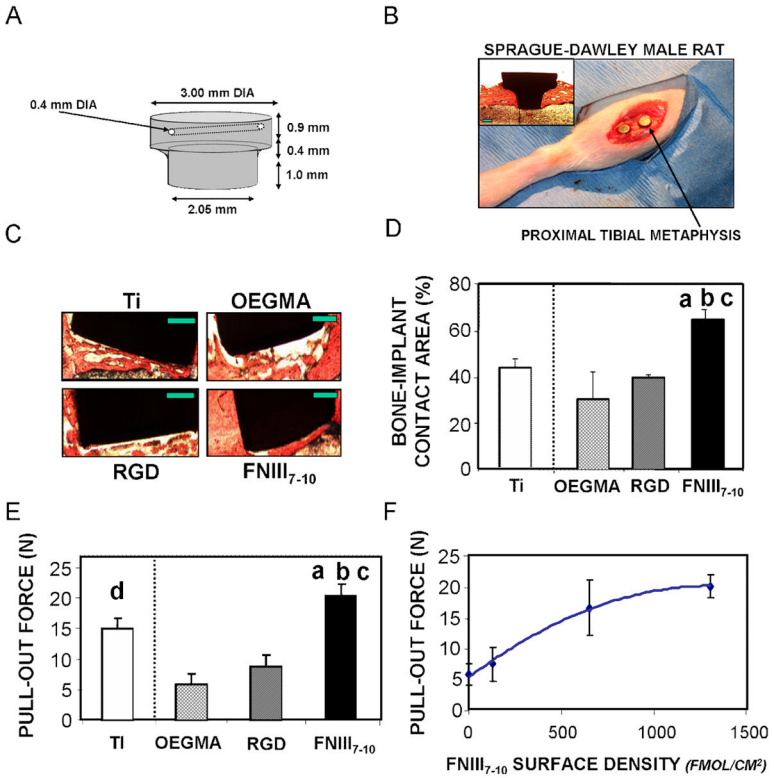

Figure 5.

Integrin specificity modulates *in vivo* implant osseointegration. (A) Schematic of tapered titanium implant used in rat tibia implant model. (B) Photograph showing placement of implants in rat tibia. Two implants were placed in each tibia. Inset micrograph is of longitudinal section of entrenched implant after 4 wk implantation, stained with Sanderson's Rapid Bone Stain™ and van Gieson counterstain. (C) Histological sections at 4 weeks post-implantation showing bone (orange)-implant (black) contact (scale bar 0.5 mm). $FNIII_{7–10}$-tethered implant surfaces displayed greater bone tissue formation and connectivity compared to other surface treatments. (D) Bone-implant contact area. a vs. RGD ($p<0.02$); b vs. Ti-serum ($p<0.02$); c vs. poly(OEGMA) ($p<0.02$). (E) Functional osseointegration as determined by pull-out force. a vs. RGD ($p<0.009$); b vs. Ti-serum ($p<0.05$); c vs. poly(OEGMA) ($p<0.001$); d vs. poly (OEGMA) ($p<0.01$). (F) Functional osseointegration increases with $FNIII_{7–10}$ tethered density (hyperbolic fit, $R^2 = 0.87$).